

## INFRARED AND RAMAN SPECTROSCOPY OF SOME FERROELECTRIC PEROVSKITE FILMS AND CERAMICS

J. Petzelt\*, T. Ostapchuk

Institute of Physics, Acad. Sci. CR, Na Slovance 2, 182 21 Praha 8, Czech Republic

The problem of reduced dielectric response in thin films compared with single crystals is addressed for SrTiO<sub>3</sub> using far infrared and micro-Raman spectroscopy. It is shown that the soft-mode behaviour, which is responsible for the dielectric response, is extremely sensitive to the film quality. In epitaxial films the stress from the substrate, which can easily change the phase diagram (e.g. induce ferroelectricity), plays the most decisive role. In polycrystalline films and ceramics, grain boundaries and possible nano-cracks, treated using the brick-wall model, can explain the observed dielectric behaviour. Soft-mode behaviour in many other perovskite films and ceramics from the BST and PZT systems is briefly discussed. In the case of PbZrO<sub>3</sub> ceramics, the effect of nano-cracks on the dynamic dielectric response is studied experimentally and explained by the brick-wall model.

(Received July 11, 2003; accepted July 31, 2003)

*Keywords:* Ferroelectric soft mode, Dielectric function, Far-infrared spectroscopy, Raman spectroscopy; Ferroelectric thin films, Ferroelectric ceramics

### 1. Introduction

In modern microelectronics there is demand for new high dielectric permittivity and low loss materials, particularly in a thin film form at high frequencies of the order of 1 GHz [1]. It is well known, however, that the dielectric properties of ferroelectric or incipient ferroelectric thin films differ pronouncedly from those of bulk single crystals. Dielectric permittivity is usually strongly reduced, less temperature dependent and the phase transitions existing in bulk crystals are smeared [2]. It is much less recognized that the similar features in lesser extend apply also to some bulk ceramics.

The dielectric response in high-permittivity perovskites is dominated by a strong low-frequency polar phonon mode, which in the case of displacive phase transition softens towards the ferroelectric or antiferroelectric phase transition (soft mode) [3, 4]. Naturally the question arises how the reduction of permittivity affects the soft-mode behaviour. We have investigated this effect using far-infrared (FIR) and Raman spectroscopy on various ferroelectric perovskite thin films and ceramics.

Infrared (IR) spectroscopy on bulk materials is a well-established technique, which in the case of strong polar modes (i. e. opaque samples) utilizes the specular normal reflection measurements on a flat polished surface, performed usually using Fourier transform (FT) interferometers. The measured power reflectance is then fitted with simple model dispersion formulae like those for a sum of classical damped oscillators or generalized four parameter oscillators in the factorized form to obtain the complex dielectric function [5]. Problems with the measurement accuracy appear in the very long wavelength IR range (below ~50 cm<sup>-1</sup>) where the conventional sources are very weak. Two other techniques have been developed to overcome this drawback: tunable monochromatic spectrometry based on backward wave oscillator (BWO) sources [6] and time domain THz spectroscopy (TDTS) based on femtosecond pulsed lasers [7]. Both techniques are phase-sensitive in the transmission mode, the latter one also in the reflection mode [8], and therefore the complex dielectric function can be calculated directly without model fitting. Moreover, these sources are by several orders of magnitude

---

\* Corresponding author: petzelt@fzu.cz

stronger than the high-pressure Hg lamp in FT spectrometers in the range of about 5-50  $\text{cm}^{-1}$ , where they are mostly used to complement and adjust the broad spectral range FT spectra (measured up to typically 4000  $\text{cm}^{-1}$  where the phonons or vibrations in non-crystalline solids cease to absorb). These novel techniques enable accurate measurements in the difficult FIR- and mm-wavelength range where many interesting absorption processes occur [6].

In the case of ferroelectric and related thin films, the main progress in the FIR spectroscopy was achieved during the recent years in our Department where we developed the evaluation method of standard transmission FT spectroscopy [9, 10] as well as TDS [10]. Due to the strong oscillator strength of the ferroelectric soft mode, the film thickness in the order of 0.1-1  $\mu\text{m}$  is just suitable for transmission measurements provided the substrate is transparent (sapphire, quartz, fused silica, pure Si, MgO, LaAlO<sub>3</sub>) and no electrode is used. All three techniques used for bulk materials can be successfully used also for such thin films.

Raman spectroscopy is a most frequently used standard technique for characterizing the lattice-vibrational properties of bulk crystals. In the case of ceramics and films usually the back-scattering geometry is used and for thin films the micro-Raman spectroscopy is much more efficient, because the focus is about 1  $\mu\text{m}$ , of the same order as the film thickness. On the other hand, for bulk ceramics the micro-Raman spectra may depend on the orientation of the studied grain and therefore for averaging over the grain orientation, the conventional Raman equipment with a large focus might be more suitable. The specific feature of Raman spectra in perovskites is the restrictive selection rules, which do not allow one-phonon activity in the simple cubic phase. Therefore the soft mode might be activated only in the distorted (e. g. ferroelectric) phase and its strength is therefore weak, comparable to the second-order spectra and it might be difficult to separate both types of the spectra to make an unambiguous assignment.

In this paper we will briefly review the results achieved on perovskite films and ceramics using the above-mentioned techniques. Our earlier work was already discussed in several reviews [9-12]. The most interesting recent results were obtained on SrTiO<sub>3</sub> (STO) ceramics and films where the soft mode behaviour is extremely sensitive to the sample quality and differ dramatically from that in single crystals [13, 14].

## 2. SrTiO<sub>3</sub> ceramics

The reason of studying the soft-mode behaviour and dielectric response of STO ceramics in comparison with those of single crystals is to study the effect of grain boundaries itself [13]. This effect also influences the behaviour of polycrystalline films, but there it can be hardly distinguished from the stress and dead-layer effects. We studied a very dense (98.8 % of theoretical density) STO ceramics, stoichiometric, nominally pure (all impurities below 0.25 %) with the grain size of 1-2  $\mu\text{m}$ , prepared by the conventional mixed-oxide route. The standard dielectric measurements up to 1 MHz revealed the same behaviour like in single crystals above ~50 K, but slower increase on further cooling with the saturation at  $\epsilon \approx 10,000$  below 10 K instead of ~25,000 in single crystals. Microwave waveguide measurements at 36 GHz performed at 100-300 K brought the same values as at low frequencies so that, like in pure single crystals, no appreciable dielectric dispersion can be expected below the soft mode response.

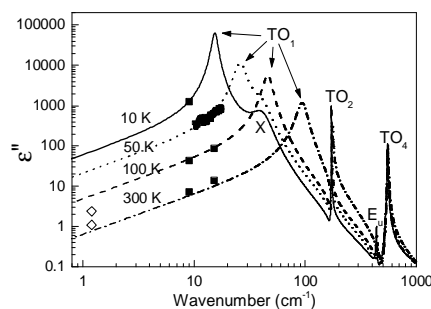


Fig. 1. Loss spectra of STO ceramics at selected temperatures calculated from the fits to FIR reflectivity (lines) together with the BWO transmission and MW data (full squares and open diamonds, respectively). After Ref. [13].

FTIR reflectivity on polished and then etched surface of a thick sample was joined with BWO reflectivity measurements in the range of 15-25  $\text{cm}^{-1}$  (0.5-0.8 THz) and BWO transmission measurements at 8-15  $\text{cm}^{-1}$  on a thin ( $d = 24 \mu\text{m}$ ) plane-parallel platelet in the 10-300 K temperature range. The resulting spectra were fitted with a factorized form of the dielectric function [5, 13] and the resulting imaginary parts (loss spectra) are shown in Fig. 1. In addition to the three IR active  $\text{TO}_1$ ,  $\text{TO}_2$ ,  $\text{TO}_4$  modes, at low temperatures also an expected  $E_u$  mode at 435  $\text{cm}^{-1}$  appears stemming from the R-point of the Brillouin zone due to the unit cell doubling below the antiferrodistortive transition at  $T_a = 132 \text{ K}$  in our ceramics (compared to  $T_a \approx 107 \text{ K}$  in single crystals) and an unexpected X mode near 40  $\text{cm}^{-1}$  which we assign to the  $E_g$  component of the structural soft-mode doublet, allowed only in the Raman spectra in centro-symmetric structure. Our detailed Raman measurements confirmed this assignment and, moreover, revealed the IR active  $\text{TO}_1$ ,  $\text{TO}_2$  and  $\text{TO}_4$  modes, Raman forbidden in the centro-symmetric structures. Their strengths increased exponentially on cooling, but their traces were seen up to the room temperature (see Fig. 2).

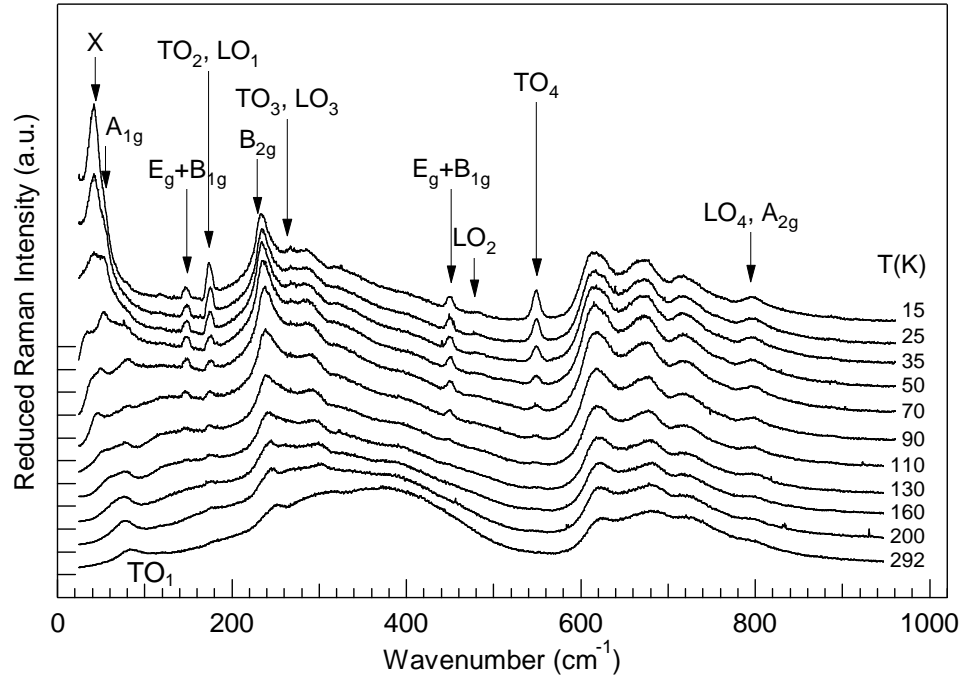


Fig. 2. Unpolarized Raman spectra of STO ceramics at selected temperatures.

The explanation is based on the obvious feature that the grain boundaries are associated with a frozen dipole moment (polarization). This polarization penetrates into the grain bulk with a characteristic correlation length proportionally to some power of the permittivity or the reciprocal soft-mode frequency,  $\xi \propto \epsilon^{d/2} \propto \omega_{\text{TO}_i}^{-d}$ , causing a non-zero mean polarization which breaks the inversion center and selection rules for IR and Raman activity. The exponent  $d$  depends on the dimensionality of polarization penetration from the polar boundary ( $d = 1$  for polar surfaces,  $d = 2$  for edges and  $d = 3$  for corners). Our experiment yields a reasonable average value  $d = 1.6$  obtained from the temperature dependence of the  $\text{TO}_1$ ,  $\text{TO}_2$  and  $\text{TO}_4$  Raman mode strengths. The polar grain boundaries could be also in origin of the reduced permittivity and mode softening at low temperatures. Namely, the local soft mode in the polar grain-boundary region is stiffened and therefore the permittivity reduced. This can be in the simplest way described by so called brick-wall model [15] which for the effective dielectric function yields

$$1/\epsilon(\omega) = (1-x)/\epsilon_{sc}(\omega) + gx/\epsilon_{gb}(\omega) \quad (1)$$

where  $\epsilon_{sc}(\omega)$  is the dielectric function in the grain bulk assumed to be equal to that of single crystals,  $\epsilon_{gb}(\omega)$  is the reduced dielectric function in the grain-boundary region of relative volume  $x \propto \xi^d$  and

$0 < g < 1$  is a geometrical factor accounting for the part of grain boundaries which is statistically in series with the bulk capacities. The remaining part in parallel with the bulk capacities is neglected for non-conducting boundaries. This approach is justified as long as the electric field is homogeneous in individual grains, i.e. the wavelength of the ac electromagnetic probe in the ceramics must be much larger than the grain size ( $\sim 1 \mu\text{m}$ ). This means that it can be safely used up to the soft-mode response including it. Mathematical analysis of the effective dielectric function shows that it keeps its form of the damped oscillator response, but the square of its eigenfrequency as well as the damping is shifted up by an amount proportional to  $\xi(T)$ . This qualitatively explains all our experimental data including stiffening of the effective soft mode at low temperatures (from  $10.7$  to  $15 \text{ cm}^{-1}$ ).

### 3. SrTiO<sub>3</sub> thin films

First FIR measurement of the soft mode response in STO films was performed in our laboratory [16]. A strong stiffening of the soft mode frequency compared with single crystals was revealed particularly below  $T_a$ . This finding was repeated also on epitaxial films using FIR ellipsometry [17] and on several other STO films in our laboratory, but remained essentially unexplained until recently [14]. In this last experiment [14] we thoroughly investigated 3 films (STO1,2,3) on (0001)-oriented sapphire substrate. STO1 was MOCVD grown with thickness 290 nm, quasi-epitaxial with a perfect (111) texture, but  $\sim 100$  nm columnar grains with two in-plane orientations differing by  $60^\circ$  [18]. Its tensile strain of  $1.7 \times 10^{-3}$  was fully due to smaller thermal expansion of the substrate compared to STO, not due to lattice mismatch, which was quite large (13%) and of opposite sign. The CSD STO2 and 3 films were polycrystalline and almost without texture, with a similar columnar grains of  $\sim 100$  nm. Both films differed only by the thickness, 360 and 720 nm, respectively, and their tensile strain was smaller than in STO1,  $1.0$  and  $0.4 \times 10^{-3}$ , respectively. However, SEM picture revealed many pores along the fraction of both films and careful optical microscopy and AFM revealed a network of nano-cracks along some of the grain boundaries in the thicker film with the characteristic distance of  $10 \mu\text{m}$  and estimated thickness of several nm. The last feature appeared to be substantial for the explanation of the dielectric response in both films.

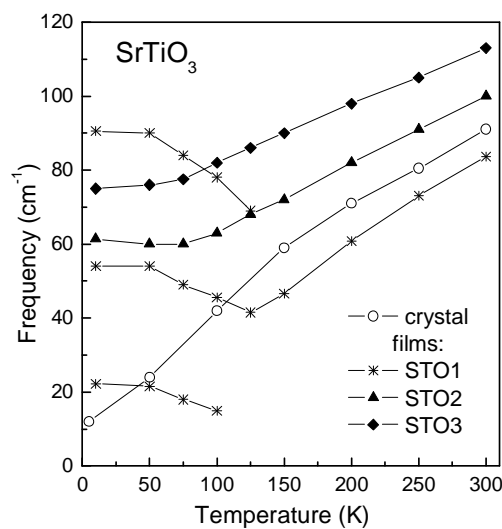


Fig. 3. Temperature dependence of the soft-mode eigenfrequencies of the three STO films in comparison with that of single-crystal. Note the appearance of new modes in the case of quasi-epitaxial STO1 film, assigned to the antiferrodistortive structural soft-mode doublet. From Ref. [10].

The FT FIR combined with BWO transmission spectroscopy in the range of  $7$ - $200 \text{ cm}^{-1}$  revealed a clear phase transition near  $125 \text{ K}$  in STO1 connected with an apparent splitting of the  $\text{TO}_1$

soft mode, but only monotonic changes in STO2 and STO3. The corresponding eigenfrequencies for all three films compared with our single-crystal data [16] are plotted in Fig. 3. STO1 shows a lower frequency than the single crystal above the phase transition, which indicates a greater tendency to ferroelectricity of the former. We interpret splitting below the transition as activation of the structural soft mode doublet allowed in non-centrosymmetric phase. Therefore we assume that the first order transition near 125 K is due to triggered antiferrodistortive and ferroelectric order parameters. A coupled mode analysis of the soft-mode triplet shows that the IR strengths of the lowest and highest-frequency mode are taken from the middle ferroelectric soft mode. The picture is supported also by micro-Raman data showing clearly the appearance of IR modes below 125 K. The possibility of such a combined ferroelectric and antiferrodistortive phase transition in thin films was predicted also theoretically [19].

STO2 and 3 films show higher soft-mode frequencies than those of single crystal in the whole temperature range and leveling off below  $\sim 100$  K like in previous measurements. The most striking feature is the further soft-mode stiffening in the thicker film compared to the thinner one. Since both the films were prepared under identical conditions, the only explanation for it is the effect of cracks, which are better developed in STO3. We analyzed the effect of nano-cracks using the brick-wall model (Eq. 1), in which instead of grain boundaries we considered air gaps ( $\epsilon_{gb}(\omega) = 1$ ) and taking  $g = 1/2$  for the columnar grain geometry. The results for the effective permittivity and soft-mode frequency are plotted in Fig. 4. It is seen, that our experimental findings for STO2 and 3 are compatible with the porosity of 0.2 and 0.4 %, respectively, independent of temperature. Such a small porosity is compatible with the average crack thickness below 10 nm in STO3, where the network of cracks was observed. However, it should be taken into account that also usual grain boundaries may play the role in the same direction due to its polar structure in analogy with ceramics. But their effect should be about the same in both STO2 and 3, because their grain size is the same. The polar structure of grain boundaries was again confirmed by micro-Raman spectra, which show the forbidden IR modes in both the films up to the room temperature and stronger than in the ceramics.

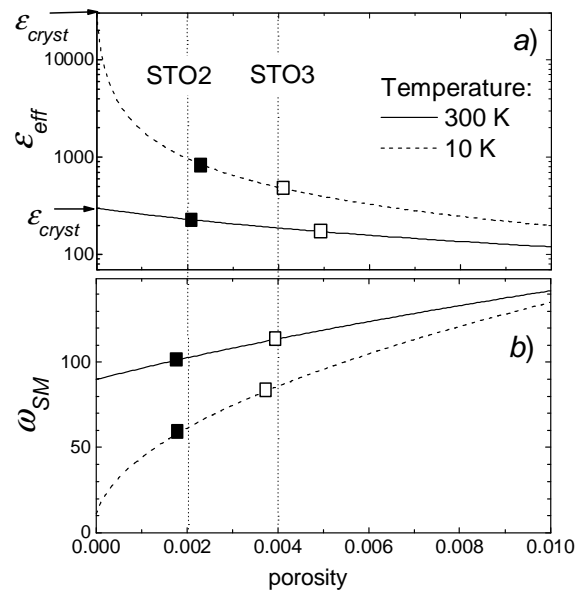


Fig. 4. Effective permittivity (a) and soft-mode frequency (b) of the STO films as functions of the volume fraction of the percolated porosity. Such kind of porosity may be present in polycrystalline films as well as in ceramics in the form of inter-grain nano-cracks. The curves are calculated using the brick-wall model. The squares represent the experimental values. From Ref. [10].

Concluding this paragraph, the main reason for the reduced dielectric response in epitaxial STO films is the possible change of the phase diagram, which often allows for ferroelectricity simultaneously with the structural distortion. Then the ferroelectric soft-mode stiffening is also caused by its coupling with the structural soft-mode doublet which hardens on cooling. In polycrystalline STO films the main effect is caused by polar grain boundaries and possible nano-cracks along some of them, which are formed to relax the tensile strains, particularly in thicker films.

#### 4. BaTiO<sub>3</sub> and BST thin films and ceramics

In the case of BaTiO<sub>3</sub> (BTO) and Ba<sub>0.1</sub>Sr<sub>0.9</sub>TiO<sub>3</sub> (BST) we studied fully analogical set of samples as in the case of STO, i.e. ceramics and three films on the (0001) sapphire substrate, one quasiepitaxial MOCVD and two polycrystalline CSD films differing just by the thickness [12, 20]. In these cases the differences among the samples of the same composition were not so pronounced and clear. To understand better the low-frequency IR and Raman spectra, let us first briefly review our understanding of the soft-mode behaviour in BTO crystals.

In its paraelectric phase (above  $T_c \approx 395$  K) the BTO lattice dynamics is strongly anharmonic, of mixed displacive and order-disorder nature, and the soft mode is overdamped [21]. The question about additional dielectric dispersion of the central-mode type near  $T_c$  below the soft mode is still under debate [4, 22]. In the tetragonal phase below  $T_c$ , the triply degenerate soft mode suddenly splits into very distant components ( $A_1$  and E components near 250 and 50 cm<sup>-1</sup>, respectively [21]) and the dielectric anisotropy becomes very high (clamped  $\epsilon_a \epsilon_c \approx 30$  at room temperature). The strong  $\epsilon_a$  response is fully due to the overdamped E-component of the soft mode, which continues slightly in its softening down to the tetragonal-orthorhombic transition near 280 K. At this transition, the doubly degenerate E-component again suddenly splits into  $B_1$  (~250 cm<sup>-1</sup>) and overdamped  $B_2$  (~60 cm<sup>-1</sup>) components. Finally, at the orthorhombic-rhombohedral transition near 190 K,  $B_1$  and  $B_2$  components change into underdamped doubly degenerate E-component of the stiffened frequency ~250 cm<sup>-1</sup>. The totally symmetric  $A_1$  component stays near 270 cm<sup>-1</sup> across all the transitions. This complex soft-mode behaviour can be understood within the framework of eight-site order-disorder model [23], in which the phase transitions consists of gradual ordering of the Ti ions [24]. In this picture, the overdamped soft component corresponds to the Ti-hopping motion among equivalent disordered sites (four and two in the tetragonal and orthorhombic phase, respectively), whereas the high-frequency components correspond to oscillations in single potential minima. Finally, in the fully ordered rhombohedral phase all (i.e. two) soft-mode components become stiffened. However, it should be noticed that since in the orthorhombic and rhombohedral phase it is not possible to prepare BTO samples in a single domain state, the above numbers are not very accurate and the conclusions should be treated merely qualitatively.

Our IR and Raman spectra on BTO ceramics, including nano-grained ceramics with the mean grain size of 50 and 100 nm, show that all the three phase transitions remain present as in crystals [25]. The difficulty with evaluation of IR spectra consist in the very strong dielectric anisotropy of the individual principal dielectric responses in the ferroelectric phases. Therefore the spectra fitting must be performed using some effective medium approximation, which assumes a simplified form of individual domains (in large-grained ceramics) or grains (in nano-grained ceramics where the grains are probably single domain) [26]. Also the interpretation of Raman spectra in ceramics (as well as in polycrystalline films) is more complex and needs to consider the directional dispersion of phonon branches [27]. So, unlike it is commonly done, the comparison of peaks in the IR and Raman response of polycrystals with non-centrosymmetric grains and their assignment should be done with a great caution.

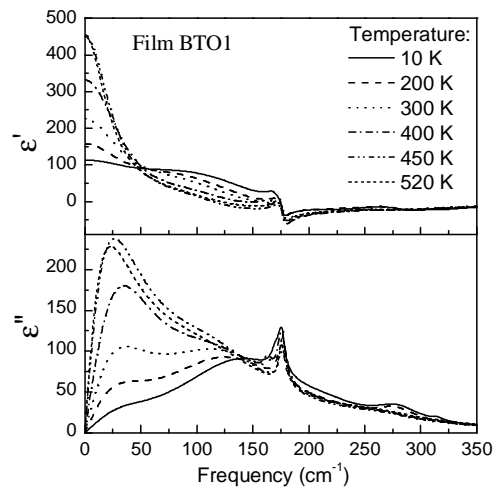


Fig. 5. Real and imaginary part of the dielectric function of the quasi-epitaxial BTO film at selected temperatures obtained from the fit to FIR and BWO transmission spectra. From Ref. [20].

In Fig. 5 we present the dielectric spectra obtained from the classical multi-oscillator fit to the transmission in unpolarized light of the quasi-epitaxial BTO film (thickness 200 nm). Since the film is well (111) oriented, the spontaneous polarization in the tetragonal and orthorhombic phase is neither in the film plane, nor perpendicular to it. The dominant spectral feature is the lowest peak near  $30 \text{ cm}^{-1}$  whose strength decreases on cooling, but remains weakly present down to 10 K. It can be assigned to the lowest soft-mode component and its presence at low temperatures means that at least part of the film has not transformed into the fully ordered rhombohedral phase. The broad absorption in the  $100\text{--}200 \text{ cm}^{-1}$  range corresponds probably to so-called geometrical resonances connected with the up-shifted soft mode due to strong depolarization fields acting at grain boundaries of strongly anisotropic grains [28, 15]. The sharp peak near  $175 \text{ cm}^{-1}$  obviously belongs to the  $\text{TO}_2$  mode and the weak feature near  $275 \text{ cm}^{-1}$  to the stiffened soft-mode component. It appears that all the phase transitions are present, but smeared with some coexistence of phases. Our Raman spectra confirm this picture.

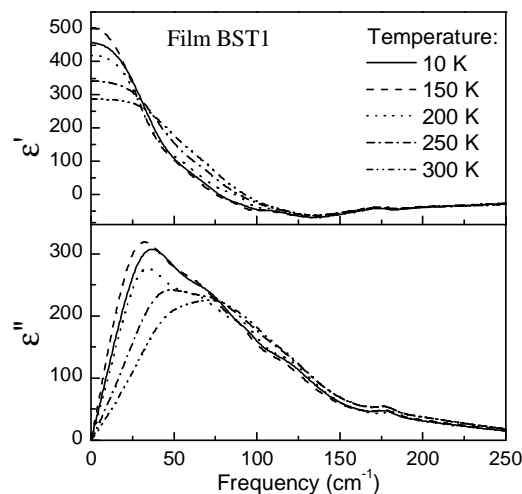


Fig. 6. Real and imaginary of the dielectric function of the quasi-epitaxial BST film at selected temperature obtained from the fit to FIR and BWO transmission spectra. From Ref. [20].

In Fig. 6 we present the dielectric spectra obtained similarly from the fit to transmission of quasi-epitaxial BST film (thickness 420 nm). One can see very broad spectra exhibiting softening down to  $\sim 40 \text{ cm}^{-1}$  near 150 K where apparently a ferroelectric transition occurs. The shift up of  $T_c$  compared with ceramics ( $T_c \approx 80 \text{ K}$ ) is obviously due to the tensile strain of  $1.11 \cdot 10^{-3}$  [18]. Based on our Raman data, it appears that the antiferrodistortive deformation coexists with the ferroelectricity, as in the STO1 film. This is not the case in BST ceramics where it was shown that the appearance of the antiferrodistortive phase (existing up to 9.4 % of Ba) is incompatible with the appearance of long-range ferroelectricity existing at higher Ba concentration [29]. In thin films again, the phase diagram could be substantially modified, as predicted theoretically [30] and recently observed for  $\text{Ba}_{0.7}\text{Sr}_{0.3}\text{TiO}_3$  [31].

## 5. Perovskite thin films and ceramics based on PZT

Our data concerning  $\text{PbTiO}_3$  and PZT 53/47 and 75/25 films are the first published FIR data on ferroelectric thin films [32]. Later on we published also FIR data on ceramics and films of relaxor PLZT 8/65/35 [33], 9.5/65/35 [34] and antiferroelectric PLZT 2/95/5 [33] and  $\text{PbZrO}_3$  [35]. These data were already reviewed [11]; therefore we mention here only that in all these cases a strong polar mode in the  $50\text{-}90 \text{ cm}^{-1}$  range was observed (sometimes split) which plays the role of the ferroelectric soft mode. In the case of PZT and relaxor PLZT it was overdamped and showed the tendency to soften towards a high temperature (about 650 K) called Burns temperature in the case of relaxors. The differences between ceramics and thin films were not so pronounced as for the BST system, but for overdamped modes our quantitative conclusions are less accurate and reliable high-temperature data are still missing. Except for  $\text{PbTiO}_3$ , the essential feature which differs from STO and BTO consists in appearance of a strong microwave and lower-frequency dielectric dispersion below the soft-mode response. It is connected basically with the dynamics of polar nano-clusters known to appear in these compounds. Therefore the static dielectric response and anomalies in these materials are much higher than the dielectric soft-mode contribution. In thin films generally this dispersion is partially blocked so that the permittivity values are again much smaller than in the corresponding ceramics, but the differences in the soft-mode behaviour are not so pronounced. The effect of crack-type porosity was recently studied on  $\text{PbZrO}_3$  ceramics [36]. Two types of dense (98 %) ceramics were studied, one of them exhibiting nano-cracks along some of grain boundaries. Its permittivity near  $T_c \approx 510 \text{ K}$  was several times smaller and the effect in the whole measured temperature range 300-550 K could be explained by  $\sim 0.3 \%$  of nano-crack-type porosity using the brick-wall model. In the dielectric spectra, the main contribution to the large permittivity peak at  $T_c$  is due to a central-mode type relaxation in the  $10^{10} \text{ Hz}$  range [37]. The relaxation frequency in the effective dielectric response of the cracked ceramics is, however, shifted up by a factor of 4, whereas the soft-phonon frequency is not appreciably affected.

### Acknowledgements:

Authors are grateful to numerous collaborators for the samples, experimental and theoretical help. The work was supported by Czech grants (projects Nos. 202/01/0612, 202/02/0238, A1010213, OC 525.20/00, AVOZ-010-914, and K 1010104).

### References

- [1] K. Uchino, *Ferroelectric Devices*, Marcel Dekker, New York (2000).
- [2] R. Waser, *Integr. Ferroelectr.* **15**, 39 (1997).
- [3] M. E. Lines, A. M. Glass, *Principles and Application of Ferroelectric and Related Materials*, Clarendon Press, Oxford (1977).
- [4] J. Petzelt, G. V. Kozlov, A. A. Volkov, *Ferroelectrics* **73**, 101 (1987).
- [5] F. Gervais, in *Infrared and Millimeter Waves* **8**, ed. K. J. Button, Academic Press, New York, 279 (1983).

- [6] G. Kozlov, A. Volkov, in *Millimeter and Submillimeter Spectroscopy*, ed. G. Gruner, Springer, Berlin, 51 (1998).
- [7] M. C Nuss, J. Orenstein, in *Millimeter and Submillimeter Wave Spectroscopy of Solids*, ed. G. Gruner, Springer, Berlin (1998).
- [8] A. Pashkin, M. Kempa, H. Nemeč, F. Kadlec, P. Kuzel, *Rev. Sci. Instr.*, in press.
- [9] J. Petzelt, T. Ostapchuk, *Ferroelectrics* **249**, 81, (2001).
- [10] J. Petzelt, P. Kuzel, I. Rychetsky, A. Pashkin, T. Ostapchuk, *Ferroelectrics*, in press.
- [11] J. Petzelt, T. Ostapchuk, S. Kamba, in *Defects and Surface-Induced Effects in Advanced Perovskites*, NATO Sci. Ser. 3, High Technol. **77**, ed. G. Borstel et al., Kluwer, 233 (2000).
- [12] J. Petzelt, T. Ostapchuk, *Ferroelectrics* **267**, 93 (2002).
- [13] J. Petzelt, T. Ostapchuk, I. Gregora, I. Rychetsky, S. Hoffmann-Eifert, A. V. Pronin, Y. Yuzyuk, B. P. Gorshunov, S. Kamba, V. Bovtun, J. Pokorny, M. Savinov, V. Porokhonsyy, D. Rafaja, P. Vanek, A. Almeida, M. R. Chaves, A. A. Volkov, M. Dressel, R. Waser, *Phys. Rev. B* **64**, 184111 (2001).
- [14] T. Ostapchuk, J. Petzelt, V. Zelezny, A. Pashkin, J. Pokorny, I. Drbohlav, R. Kuzel, D. Rafaja, B. P. Gorshunov, M. Dressel, Ch. Ohly, S. Hoffmann-Eifert, R. Waser, *Phys. Rev. B* **66**, 235406 (2002).
- [15] I. Rychetsky, J. Petzelt, T. Ostapchuk, *Appl. Phys. Lett.* **81**, 4224 (2002).
- [16] I. Fedorov, V. Zelezny, J. Petzelt, V. Trepakov, M. Jelinek, V. Trtik, M. Cernansky, V. Studnicka, *Ferroelectrics* **208-209**, 413 (1998).
- [17] A. A. Sirenko, C. Bernhard, A. Golnik, A. M. Clark, J. Hao, W. Si, X. X. Xi, *Nature* **404**, 373 (2000).
- [18] D. Rafaja, J. Kub, D. Simek, J. Lindner, J. Petzelt, *Thin Sol. Films* **422**, 8 (2002).
- [19] N. A. Pertsev, A. K. Tagantsev, N. Setter, *Phys. Rev. B* **61**, R825 (2000); *ibid.* **65**, 219901(E) (2002).
- [20] J. Petzelt, T. Ostapchuk, A. Pashkin, I. Rychetsky, *J. Eur. Ceram. Soc.*, in press.
- [21] Y. Luspín, J. L. Servoin, F. Gervais, *J. Phys. C: Sol. St. Phys.* **13**, 3761 (1980).
- [22] H. Vogt, A. Sanjurjo, G. Rossbroich, *Phys. Rev. B* **26**, 5904 (1982).
- [23] R. Comes, M. Lambert, A. Guinier, *Sol. State Commun.* **6**, 715 (1968).
- [24] T. P. Doherty, G. P. Wiederrecht, K. A. Nelson, M. H. Garrett, H. P. Jenssen, C. Warde, *Phys. Rev. B* **50**, 8996 (1994).
- [25] L. Mitoseriu et al., to be publ.
- [26] C. Pecharroman, J. E. Iglesias, *J. Phys.: Condens. Matter* **6**, 7125 (1994).
- [27] W. Hayes, R. Loudon, *Scattering of Light by Crystals*, Wiley, New York (1978).
- [28] I. Rychetsky, O. Hudak, J. Petzelt, *Phase Transitions* **67**, 725 (1999).
- [29] C. Menoret, J. M. Kiat, B. Dkhil, M. Dunlop, H. Dammak, O. Hernandez, *Phys. Rev. B* **65**, 224104 (2002).
- [30] V. G. Koukhar, N. A. Pertsev, R. Waser, *Phys. Rev. B* **64**, 214103 (2001).
- [31] Yu. I. Yuzyuk, J. L. Sauvajol, P. Simon, V. L. Lorman et al., *J. Appl. Phys.* **93**, 9930 (2003).
- [32] I. Fedorov, J. Petzelt, V. Zelezny, G. A. Komandin, A. A. Volkov, Y. Huang, N. Setter, *J. Phys.: Condens. Matter* **7**, 4313 (1995).
- [33] T. Ostapchuk, V. Zelezny, J. Petzelt, B. Malic, M. Kosec, *Proc. SPIE* **37DP**, 156 (1999).
- [34] I. Fedorov, J. Petzelt, V. Zelezny, A. A. Volkov, M. Kosec, U. Delalut, *J. Phys.: Condens. Matter* **9**, 5205 (1997).
- [35] T. Ostapchuk, J. Petzelt, V. Zelezny, S. Kamba, B. Malič, M. Kosec, L. Cakare, K. Roleder, *J. Dec.*, *Ferroelectrics* **239**, 979 (2000).
- [36] T. Ostapchuk, J. Petzelt, I. Rychetsky, V. Porokhonsky, B. Mailc, M. Kosec, P. Vilarinho, *Ferroelectrics*, accepted.
- [37] T. Ostapchuk, J. Petzelt, V. Zelezny, S. Kamba, V. Bovtun, V. Porokhonsky, A. Pashkin, P. Kuzel, M. D. Glinchuk, I. P. Bykov, B. Gorshunov, M. Dressel, *J. Phys.: Condens. Matter* **13**, 2677 (2001).